Journal of Engineering Physics and Thermophysics, Vol. 82, No. 1, 2009

PHOTOCURRENT AMPLIFICATION EFFECT OF THE FET GATE *p–n* JUNCTION

D. M. Edgorova

UDC 621.315.592

A superlinear increase in the light current of the gate with an increase in the exciting integral light intensity (from 100 to 1000 lx) has been revealed experimentally. This superlinear increase is due to the increase in the internal gradient field generated by the minority carriers by the cutoff voltage of the gate leading to an additional interband generation of photocarriers. On the basis of the investigation of the dependence of photocurrent on the cutoff voltage it has been shown that the photocurrent increases linearly, which is explained by the creation of an internal electric field by the majority carriers of the base zone of the gate p–n junction.

Keywords: *field-effect phototransistor, p–n junction, photocurrent, amplification effect, carrier density, gradient.*

Introduction. The field-effect phototransistor with a control *p–n* junction and an open channel is an ideal model structure for investigating photoelectrical phenomena in *p–n*-homo- and heterojunctions at appropriate switching conditions, since the light striking the base zone of the FET (Fig. 1a) generates electrons and holes separated by the *p–n* junction field, as in the photodiode. The FET photosensitivity is estimated by some authors [1] as the product of the current sensitivity of the gate $S_I = I^{\text{photo}}/\Phi$ by the characteristic amplification coefficient of the transistor gR_{g}. Other authors [2, 3], basing on investigations of the dependences of gate and source photocurrents on the illumination intensity of FETs whose channel is doped with Te and simultaneously with Te and Si, came to the conclusion that in both FETs with increasing illumination intensity the ratio of the source photocurrent to the incident radiation intensity decreases by 20% from 30 to 24 μA/lx. In so doing, the dependences of photocurrents on the illumination intensity had a saturating character due to the decrease in the amplification coefficient of the transistor structures estimated as the triode-to-diode photosensitivity ratio (Fig. 1b). In the first transistor, the carrier density increases from the *p–n* junction boundary to the illuminated surface, and in the second transistor a uniform thickness distribution of the carrier density due to the increase in the degree of compensation of tellurium dopants by silicon has been obtained. As a result, the photosensitivity of the gate *p–n* junction of the FET with a tellurium-doped base zone turned out to be higher ($3.1\cdot10^{-4}$ μA/lx) than in the transistor whose base zone was doped simultaneously with Te and Si ($2\cdot10^{-4}$ μA/lx), and the photoelectric amplification coefficients defined as the triode-to-diode photosensitivity ratio turned out to be equal to 24 and 10, respectively. Consequently, to a higher diode photosensitivity there corresponds a higher transistor photosensitivity. Moreover, the considered structures turned out to be characterized by a decrease in the photosensitivity of the gate *p–n* junction with increasing optical signal intensity, which is due to the concentration of the carrier separation zone in a narrow space charge depletion layer. As a result, the gate photocurrent has also a maximum at a fixed cutoff voltage and its further increase leads to a subsequent decrease in the photosensitivity [4, 5]. This means that in this case the photocurrent amplification effect is absent and the photosignal amplification is associated with the transistor amplification coefficient which varies as the photosensitivity of the gate *p–n* junction. The development of diode and transistor structures displaying the photocurrent amplification effect and photosensitivity in a wide range of light signal intensities is of interest for optical signal processing without distortions.

The dependences of the light characteristics of the gate *p–n* junction on the illumination intensity and on the cutoff voltage have also been investigated and the physical processes leading to the photocurrent amplification effect of the gate of the field-effect phototransistor whose channel is doped with tin have been analyzed.

Physicotechnical Institute, Scientific-Production Association "Fizika–Solntse," Academy of Sciences of the Republic of Uzbekistan, 2 b Mavlyanov Str., Tashkent, 100084, Uzbekistan; email: yodgorova@uzsci.net. Translated from Inzhenerno-Fizicheskii Zhurnal, Vol. 82, No. 1, pp. 191–198, January–February, 2009. Original article submitted April 2, 2007; revision submitted January 17, 2008.

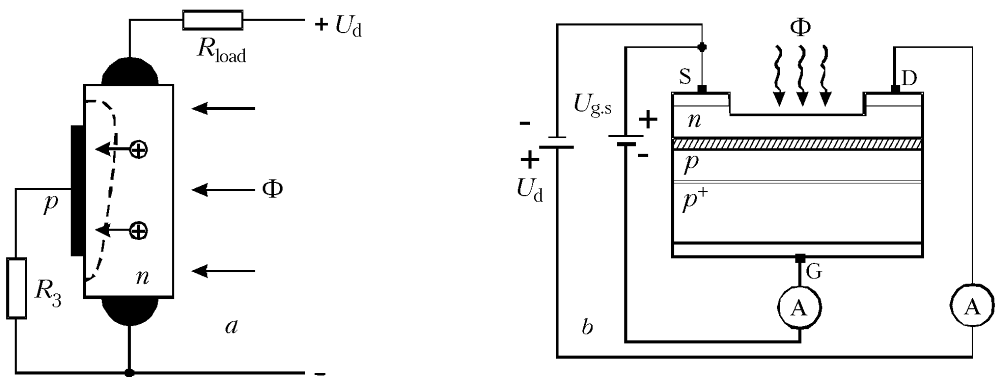

Fig. 1. Switching circuit of the field-effect phototransistor with self-bias on the gate [1] (a) and with a common source [3] (b); D, drain; S, source; G, gate.

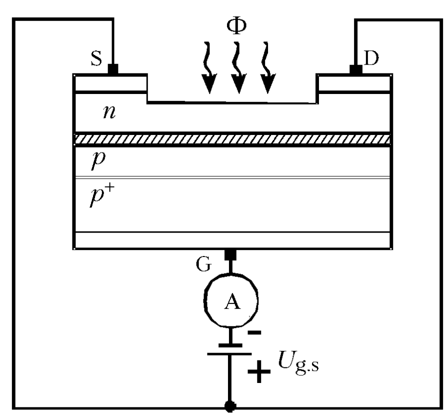

Fig. 2. Structure of the investigated GaAs field-effect phototransistor with a control p^+–p–n junction in the photodiode switching regime with connected drain and source leads; S, source; G, gate.

Experimental Specimens and Investigation of the Photoelectrical Characteristics. The investigated structures of the FET are based on step-by-step grown epitaxial layers of the *p*- and *n*-type of conduction on a highly doped p^+GaAs substrate. The control *p*–*n* junction of the FET represents a gallium-arsenide-based p^+–p–n homojunction in which the groove-channel etched in the *n*-zone serves as a photodetection window (Fig. 2). The epitaxial layer thickness under a groove of length 50 μm is 0.32 μm at a width of 700 μm. In the Sn-doped *n*GaAs channel, the carrier density decreases towards the surface from $3\cdot10^{16}$ cm^{-3} to $1\cdot10^{16}$ cm^{-3}. The drain-source contact areas of size 700 ×750 μm were formed by sequential deposition of tin and nickel on its top. The ohmic contact to the gate zone was obtained by depositing nickel to which the negative potential of the cutoff voltage was connected, and the positive potential was connected to the source contact closed with the drain, as is shown in Fig. 2, providing the photodiode regime. The voltage dependence of the dark current of the gate (Fig. 3) is described by the power law $I \sim U^{\gamma}$ creating two parts with exponents 0.6 and 1.78 (inset). In the first part where low noises are provided, the current transfer mechanism is determined by the generation of carriers in the space-charge layer, and the second part is associated with the avalanche processes. Since the carrier density in the base is two orders of magnitude higher than in the *p*-zone, with increasing cutoff voltage the space-charge layer extends into the base. For instance, as the cutoff voltage of the gate increases, the space-charge layer extends in the direction of the channel surface in the thickness (*d*) of the base zone (Fig. 4, curve 1), where corresponding carrier densities have been created. In so doing, the thickness of the space-charge layer is defined as an increment in the initial thickness $W = W_0 + \Delta W$. Here it should be noted that W is identical to *d*. The curve of the change in the carrier density in the base zone thickness determined from the capacity-voltage characteristics is linear (Fig. 4, curve 2) [6], and the contact potential difference U_c = 1.03 eV. The carrier density gradient in the channel thickness determined on the basis of the data of Fig. 4 is $\Delta N = (N_1 - N_2)/(d_2 - d_1)$ =

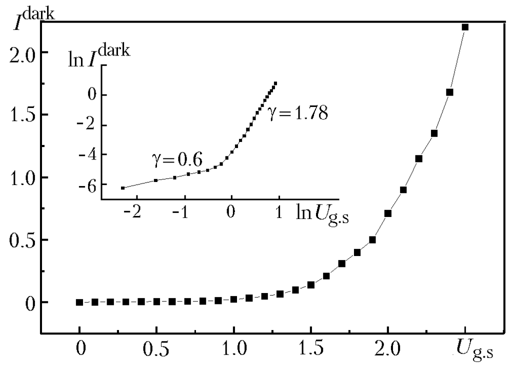

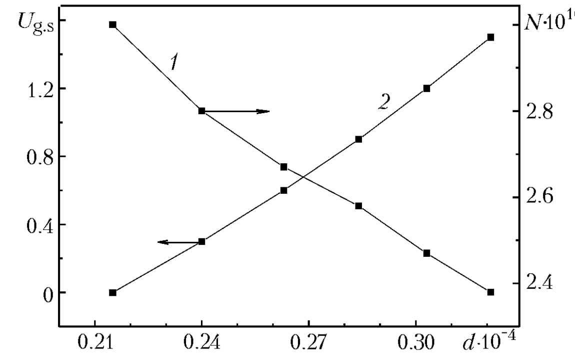

Fig. 3. Dark current of the gate p–n junction as a function of the cutoff voltage (in the inset on a double logarithmic scale). I^{dark}, μA; $U_{g.s}$, V.

Fig. 4. Majority carrier density distribution in the base thickness (1) and depletion part of the base versus the cutoff voltage of the gate p–n junction (2). $U_{g.s}$, V; d, cm; N, cm^{-3}.

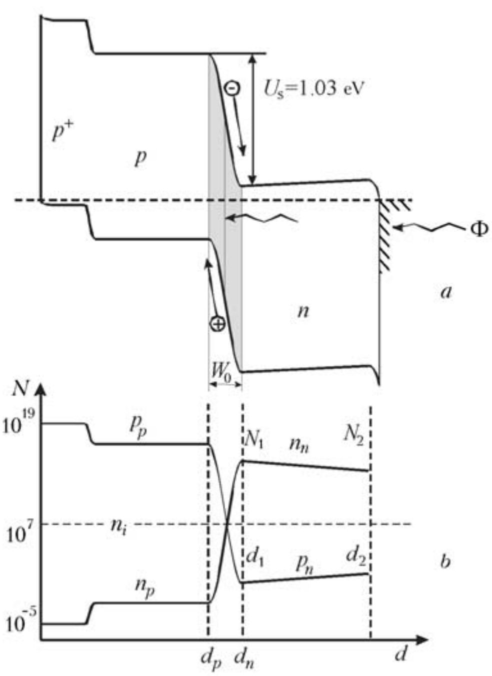

Fig. 5. Band structure of the p^+–p–n junction in the equilibrium state (a) and density distribution of carriers in the thickness (b).

$6.25{\cdot}10^{20}$ cm^{-4}, and the gradient voltage [7] is ΔU_{gr} = 1.05 V. The distributions of majority and minority carrier densities along the structure coordinate, constructed on the basis of the experimental data, as well as the band diagram in the equilibrium state are given in Fig. 5. Here the majority carrier density in the p-zone is equal to P_p and in the n-zone n_n ($n_n = N$), with the carrier density in the n-zone decreasing from N_1 to N_2 on the segment $d_2 - d_1$ to create a gradient voltage. In this case, the space-charge layer covers part d_p on the side of the p-zone and part d_n on the side of the n-zone. At their boundary we have the intrinsic carrier density n_i. In view of the law $n_i^2 = P_p n_p = P_p n_p$ [7] the created distributions of minority carrier densities, i.e., the determined concentrations of electrons n_p in the p-zone and holes P_n in the n-zone, are given in Fig. 5b. Under illumination from the side of the channel the concentration of photogenerated electrons increases directly with the radiation intensity, and the concentration of photogenerated holes compared to the dark current values increases near the space charge boundary. Investigations of the photoelectrical characteristics of this structure carried out under illumination of the channel region depending on the integral radiation have

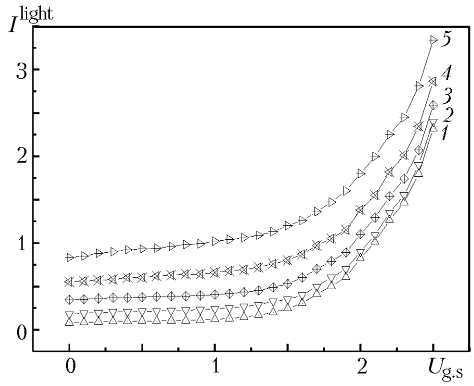

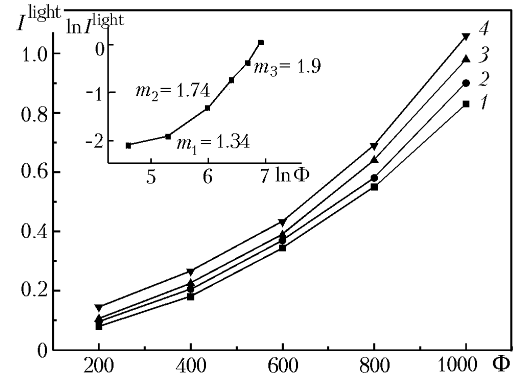

Fig. 6. Light current of the gate versus the cutoff voltage at various integral illumination intensities: 1) 200 lx; 2) 400; 3) 600; 4) 800; 5) 1000. I^{light}, μA; $U_{g.s}$, V.

Fig. 7. Light current of the gate versus the illumination intensity at cutoff voltages of 1) 0 V; 2) 0.3; 3) 0.8; 4) 1.2. I^{light}, μA; Φ, lx.

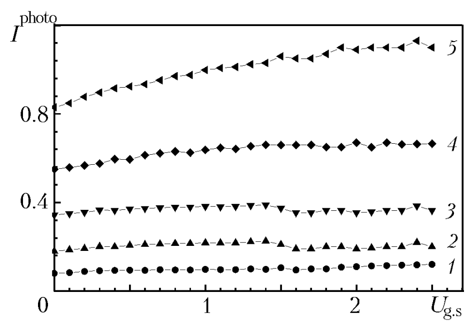

Fig. 8. Gate photocurrent versus the cutoff voltage at various integral illumination intensities: 1) 200 lx; 2) 400; 3) 600; 4) 800; 5) 1000. I^{photo}, μA; $U_{g.s}$, V.

shown that the photocurrents increase first linearly and then more intensively as the voltage is increased from 0 to 2.5 V (Fig. 6). In so doing, as the illumination intensity increases from 100 to 1000 lx, the character of the voltage-current curve remains unaltered. The dependences of light currents on the illumination intensity at cutoff voltages (0–1.2 V) corresponding to the first portion of the dark current are superlinear (Fig. 7). The exponent m of the dependence of the light current on the illumination intensity for a cutoff voltage of 0.8 V equals 1.4–2 (Fig. 7, inset) unlike *p–n* junctions with a linear light characteristic [8].

Another feature of the structure associated with the illumination intensity is a linear increase in the gate photocurrent ($I^{photo} = I^{light} - I^{dark}$) with increasing voltage (Fig. 8), and the slope of the photocurrent growth curve steepens with increasing illumination intensity. In so doing, the physical processes proceeding in the space charge-zone of the gate *p–n* junction under the action of the optical radiation and electric field can be explained with the aid of the band diagram constructed at a cutoff voltage of 0.8 V (Fig. 9a). With increasing cutoff voltage the space-charge layer begins to cover an increasingly larger part of the base zone due to the decrease in the majority and minority carrier density at the boundary with quasi-neutral zones compared to the equilibrium one. As a result, the number of generated carriers will increase directly with the depletion layer thickness, leading to an internal increase in the photocurrent, which is due to the characteristic distribution of majority and minority carriers in the base thickness in the cutoff regime of the gate (Fig. 9b).

Thus, in the *p–n* junction of the FET gate whose base zone is doped with tin with a carrier density decreasing from $3 \cdot 10^{16}$ cm^{-3} to $1 \cdot 10^{16}$ cm^{-3} from the boundary of the *p–n* junction towards the surface, as opposed to the tellurium-doped *p–n* junction [9], the voltage-current curve is nonlinear, breaking down into two segments. In the first segment up to 1.2 V the current is minimal and then increases exponentially. The light current increases superlinearly with increasing illumination intensity, and the dependence of the photocurrent on the cutoff voltage acquires a rising

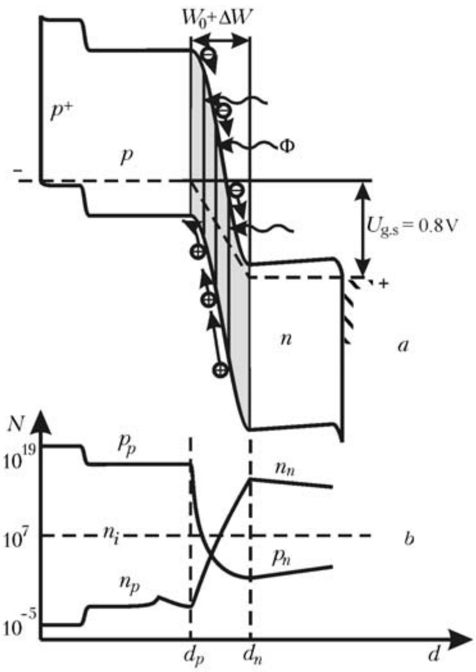

Fig. 9. Band structure of the p^+–p–n junction at a cutoff voltage of 0.8 V (a) and density distribution of carriers in the thickness (b).

character, causing an increase in the photosensitivity. In so doing, the photocurrent increases as both the radiation intensity and the operating voltage increase, i.e., amplification of the gate photocurrent takes place. In this case, the effect of photocurrent amplification is that, at a given electric amplification coefficient of the transistor, its photocurrent is increased due to an increase in the cutoff voltage and the input optical signal intensity.

Analysis of the Effect of Gate Photocurrent Amplification. It is known that in the FET a uniform distribution of dopants in the channel thickness is sought [10], and the input signal amplification is obtained by increasing the transistor amplification coefficient, i.e., the transconductance. As a result, the possibility of controlling the photoamplification properties by varying the photosensitivity of the gate *p–n* junction is overlooked. In photodiodes, the sensitivity is determined by the thickness of the depletion zone and the curve of its expansion as a function of the cutoff voltage: the thicker the space-charge zone, the higher the photocurrent [11]. Therefore, to obtain controlled sensitivity of the *p–n* junction, it is necessary to realize the physical ways of effective expansion of the depletion layer depending on the cutoff voltage. This can be done, for example, by creating a nonuniform distribution of the carrier density [12], since in the *p–n* junction with a uniform or increasing carrier density in the base the photocurrent values decrease (or remain unaltered) with increasing voltage [1]. But in our case, as is shown in Fig. 8, as the illumination intensity increases, the photocurrent increases with increasing cutoff voltage due to the presence of internal photoelectric amplification. In particular, the photosensitivity of the gate *p–n* junction increases as both the cutoff voltage for given illumination intensities (Fig. 10, curve 1) and the radiation intensity at given cutoff voltages (Fig. 10, curve 2) increase. Its value reaches $1.14 \cdot 10^{-3}$ μA/lx against $3.1 \cdot 10^{-4}$ μA/lx in the FET with a tellurium-doped channel [3]. The superlinear dependence of the light characteristics and the amplification of the photocurrent of the gate *p–n* junction observed in the experiment can be explained by the following mechanism.

At a zero voltage on the gate, illumination of the channel zone leads to the appearance of a photocurrent caused by the separation of the electron-hole pairs in the space-charge layer of the gate *p–n* junction. As the illumination intensity increases, the number of generated carriers increases due to the increase in the rate of generation of electron-hole pairs. In so doing, the Fermi quasi-level approaches the conduction band and the generated electrons in the gradient field reach the gate contact unimpeded. Under these conditions the internal electric field is concentrated in a narrow space-charge layer since in its adjoining *n*GaAs zone there is some increase (from $1.24 \cdot 10^{-2}$ cm^{-3} to $1.56 \cdot 10^{-2}$ cm^{-3}) in the minority carrier density (Fig. 5b). Further on, as the cutoff voltage increases, the space-charge

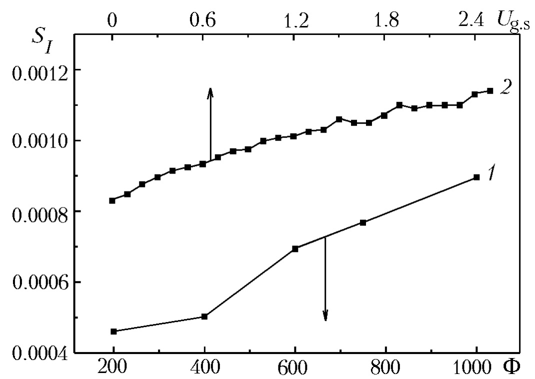

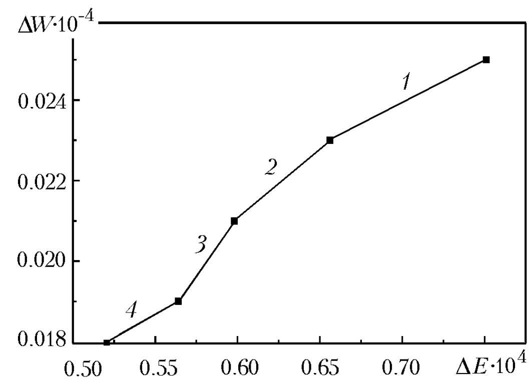

Fig. 10. Photosensitivity versus the cutoff voltage at 1000 lx (1) and the illumination intensity at a cutoff voltage of 0.3 V (2). S_I, μA/lx; Φ, lx; $U_{g.s}$, V.

Fig. 11. Thickness increment of the space-charge layer versus the electric field strength increment of the gate *p–n* junction as a junction of the given fixed voltages with a step of 0.3 V. $\Delta E\cdot 10^4$, V/cm; $\Delta W\cdot 10^{-4}$, cm.

TABLE 1. Density Distributions of Minority Carriers and Electric Field Strengths as a Function of the Modeled Thickness of the Base

$U_{g.s}$, V	$n_p\cdot 10^{-4}$, cm^{-3}	$P_n\cdot 10^{-2}$, cm^{-3}	$W\cdot 10^{-5}$, cm	$E\cdot 10^4$, V/cm	$W\cdot 10^{-6}$, cm	$E\cdot 10^3$, V/cm
0	1.24	1.24	2.15	4.79	—	—
0.3	1.32	1.42	2.40	5.54	2.50	7.51
0.6	1.39	1.57	2.63	6.20	2.30	6.56
0.9	1.45	1.69	2.84	6.804	2.10	5.98
1.2	1.50	1.82	3.03	7.36	1.90	5.64
1.5	1.54	1.94	3.21	7.88	1.80	5.22

layer will move into the zone with a gradient carrier density where, depending on the cutoff voltage, the space-charge layer begins to expand more effectively (Fig. 9a). In so doing, upon receding from the *p–n* junction boundary, the minority carrier densities of electrons in the *p*-zone and holes in the *n*-zone increase to create drift fields for photogenerated carriers, and in the cutoff regime of the gate *p–n* junction this gradient increases (Fig. 9b). As a result, effective transfer of generated electrons from the adjoining *p*-zone into the *n*-zone and of holes into the *p*-zone by the drift fields is provided.

The proposed mechanism of gate photocurrent amplification is validated by the following. For each given fixed value of the cutoff voltage ($\Delta U_{g.s}$ = 0.3 V) we obtain the corresponding increment of the the space-charge layer (ΔW) and of the electric field strength (ΔE), whose calculated data are presented in Table 1. In particular, as is shown in Fig. 11, at first, for the next fixed step of voltage, due to the positive carrier density gradient we have a considerable increment of the electric field strength compared to the the space-charge layer increment (Fig. 11, section 1). In accordance with the band diagram, the electric field of the *p–n* junction as a function of the cutoff voltage applied will increase until the gradient zone of majority carriers is reached. In the next given step of the cutoff voltage, a more effective expansion of the space-charge layer occurs and we have a smaller increment of the electric field strength compared to the previous one (Fig. 11, section 2). However, since in the direction towards the base surface from the boundary with a space-charge layer the density of majority carriers (electrons) becomes increasingly lower and the density of minority carriers (holes) — higher (Fig. 9b), the gradient of holes — of the drift field — for photogenerated holes will increase. As a result, the number of photogenerated carriers increases and their movement towards the base surface is characterized by not only diffusion but also by a drift in the accelerating electric field created by the carrier density gradient. In other words, photogenerated electrons are effectively transferred, without loss, into the channel and reach the source contact, and holes reach the gate contact (Fig. 9a), which prevents carrier recombination in the quasi-linear part of the base and leads to photocurrent amplification [11]. With further increase in the cutoff voltage (above 0.9 V) the increment of the space-charge layer thickness is retarded (Fig. 11, sections 3 and 4), and the electric field increment begins to prevail, which takes the dark current to the section of exponential growth with suppression of the photocurrent amplification effect.

Thus, from the analysis of the photoelectrical characteristics it follows that the shape of the cutoff voltage-photocurrent curve and the superlinearity of the dependence of the light current on the light intensity characterize the photocurrent amplification effect of the gate p–n junction. The gradient distribution of majority and minority carriers in the base creating internal electric fields is responsible for the photocurrent amplification effect.

Conclusions. Practically any semiconductor photodetector is used in pair with a FET for obtaining an optimal output signal. In this aspect, the investigated field-effect phototransistor, combining the functions of the photodiode and amplifier, is of interest as a universal photodetector superseding the hybrid-coupled photodiode and transistor. Doping with tin of the base zone with a carrier density distribution decreasing from $3 \cdot 10^{16}$ cm^{-3} to $1 \cdot 10^{16}$ cm^{-3} from the p–n junction boundary to the surface ensures the serviceability in a wide range of optical signal intensities and a superlinear increase in the gate photocurrent with increasing intensity of the exciting integral light (from 100 to 1000 lx) due to the establishment of a gradient drift field in the base zone of the gate p–n junction. In so doing, an increase in the cutoff voltage leads to a linear increase in the photocurrent. Such field-effect photoresistors are of interest for fiber-optical transmission systems.

NOTATION

d, base thickness coordinate; d_1, base thickness covered by the space-charge layer of the p–n junction; d_2, thickness of the quasi-linear part of the base; d_p, d_n, thicknesses of the space-charge layer on the side of the p- and n-zones; E, ΔE, electric field strength of the p–n junction and its increment, V/cm; g, FET transconductance; I, current, μA; I^{dark}, dark current, μA; I^{light}, light current under illumination, μA; I^{photo}, photocurrent between the gate and the source, μA; $\Delta I_{\text{d.s}}$, change in the drain current, μA; m, exponent of the dependence of light current on the illumination intensity; n, n-zone; n^0, high-resistance n-zone; n_i, intrinsic carrier density; n_n, majority electron carrier density; n_p, electron density in the p-zone; N, carrier density; N_1, carrier density in the base at the boundary with the space-charge layer of the p–n junction; N_2, carrier density in the base thickness; ΔN, gradient density, cm^{-4}; P_p, majority hole carrier density; P_n, hole density in the n-zone; p^+, highly doped p-zone; p, p-zone; R_{load}, load resistance, Ohm; R_{g}, resistance in the gate circuit, Ohm; S_I, photosensitivity, μA/lx; U, voltage; U_{c}, contact potential difference, eV; U_{d}, drain voltage, V; $U_{\text{g.s}}$, $\Delta U_{\text{g.s}}$, gate voltage and its change, V; ΔU_{gr}, gradient voltage, V; W_0, ΔW, initial thickness of the space-charge layer of the p–n junction and its increment, μm; γ, exponent of the dark current-voltage characteristic; Φ, illuminance, lx. Subscripts: p, holes; n, electrons; gr, gradient; g.s, gate-source; d.s, drain-source; load, load; g, gate load; c, contact; light, illumination current; photo, difference between light and dark currents; dark, current in the dark.

REFERENCES

1. I. M. Vikulin and V. I. Stafeev, *Physics of Semiconducting Devices* [in Russian], Radio i Svyaz', Moscow (1990), pp. 125–126.
2. A. V. Karimov, Field-effect phototransistor with a face gate, *Electronic Engineering*, Ser. 2, *Semiconducting Devices*, Issue 5, 93–95 (1990).
3. A. V. Karimov, *Multifunctional Gallium Arsenide Fine-Junction Structures* [in Russian], FAN, Tashkent (1992), pp. 94–99.
4. S. A. Azimov, P. M. Karageorgii-Alkalaev, A. V. Karimov, and M. Mirzabaev, Specific features of FET-type photosensitive arsenide-gallium structures, *Izv. Akad. Nauk UzSSR*, *Ser. Fiz.-Mat. Nauk*, No. 2, 44–48 (1979).
5. M. A. Abdukadyrov, A. V. Karimov, and M. Mirzabaev, Investigation of photosensitive unipolar transistors with a heterojunction, *Mikroélektronika*, **13**, No. 2, 169–170 (1984).
6. D. M. Edgorova, Influence of the characteristic distribution of Te and Sn dopants on the photoelectric characteristics of the field-effect phototransistor, *Peterburg. Zh. Élektron.*, No. 2, 69–73 (2007).
7. S. M. Sze, *Physics of Semiconductor Devices* [Russian translation], Book 2, Mir, Moscow (1984), pp. 80–91.
8. M. I. Épshtein, *Measurement of Optical Radiation* [in Russian], Énergoatomizdat, Moscow (1990), pp. 109–115.

9. V. M. Andreev, L. M. Dolginov, and D. N. Tret'yakov, *Liquid Epitaxy in the Technology of Semiconductor Devices* [in Russian], Sov. Radio, Moscow (1975), pp. 83–85.
10. A. V. Karimov, Photosensitive arsenide-gallium *p–n*-junction FETs, *Élektron. Tekhn.*, *Ser.* 11, No. 2, 111–113 (1987).
11. P. K. Cheo, *Fiber Optics* [Russian translation], Énergoatomizdat, Moscow (1988), pp. 228–233.
12. I. Aut, D. Gentsov, and K. German, *Photoelectrical Phenomena* [Russian translation], Mir, Moscow (1980), pp. 183–187.